

RESEARCH ARTICLE

Transcriptomic adaptation of skeletal muscle in response to MICT and HIIT exercise modalities

Weihaio Hong¹, Yisheng Luan¹, Jianrong Zheng², Yingzhe Xiong³, Bing Zhang^{1*}, Yixuan Ma^{1*}

1 Division of Sports Science and Physical Education, Tsinghua University, Beijing, China, **2** Department of Prevention and Early Warning Research, Guangzhou National Laboratory, Guangzhou, China, **3** School of Physical Education, Central China Normal University, Wuhan, China

* bzhang@mail.tsinghua.edu.cn (BZ); hardcandy@mail.tsinghua.edu.cn (YM)



Abstract

Skeletal muscle exhibits remarkable plasticity in response to diverse stimuli, with exercise serving as a potent trigger. Varied exercise modalities, including moderate-intensity continuous training (MICT) and high-intensity interval training (HIIT), induce distinct structural and functional adaptations on skeletal muscle. However, the underlying molecular mechanisms governing these adaptations remain poorly understood. In this study, we utilized RNA-seq to characterize the transcriptomic profile of murine gastrocnemius muscle following 8-week treadmill-based MICT (M group) and HIIT (H group). A total of 1052 DEGs were screened in H vs. M. Among the top 10 significant DEGs, *Foxo1* and *Myod1* are closely related to muscular physiology. Through KEGG pathway analysis, distinct adaptations were primarily identified in the FoxO, MAPK, and PI3K-AKT pathways. By analyzing the expression of myokines, a significantly higher *Igf-1* expression level was observed in the M group compared to the H group. Therefore, IGF-1, a well-known upstream regulator of both the PI3K-AKT-FoxO and MAPK pathways, might drive distinct muscle adaptations through variations in *Igf-1* expression induced by these two exercise modalities.

OPEN ACCESS

Citation: Hong W, Luan Y, Zheng J, Xiong Y, Zhang B, Ma Y (2025) Transcriptomic adaptation of skeletal muscle in response to MICT and HIIT exercise modalities. PLoS ONE 20(2): e0318782. <https://doi.org/10.1371/journal.pone.0318782>

Editor: Esedullah Akaras, Erzurum Technical University: Erzurum Teknik Universitesi, TÜRKİYE

Received: October 8, 2024

Accepted: January 22, 2025

Published: February 25, 2025

Copyright: © 2025 Hong et al. This is an open access article distributed under the terms of the [Creative Commons Attribution License](https://creativecommons.org/licenses/by/4.0/), which permits unrestricted use, distribution, and reproduction in any medium, provided the original author and source are credited.

Data availability statement: All relevant data are within the paper and its [Supporting information](#) files.

Funding: The author(s) received no specific funding for this work.

Competing interests: The authors have declared that no competing interests exist.

Introduction

Skeletal muscle is a dynamic and versatile tissue capable of adapting to functional demands imposed by a myriad of internal and external stimuli [1]. Among these stimuli, exercise serves as a potent trigger, inducing a cascade of physiological changes within skeletal muscle [2–4]. Such changes encompass alterations in contractile machinery, structural organization, and metabolic pathways within muscle fibers. Additionally, exercise enhances capillary density and promotes the remodeling of connective tissue. Together, these processes underpin skeletal muscle adaptations that are closely linked to the specific type of exercise undertaken [5,6].

Among the various exercise modalities, moderate-intensity continuous training (MICT) and high-intensity interval training (HIIT) are two exercise modalities with distinct characteristics and benefits [7]. MICT involves moderate-intensity, long-duration aerobic activities such as jogging, cycling, or swimming, typically lasting over 30 minutes. This approach is

avored for its safety, stability, and ease of adherence, rendering it effective in improving cardiovascular endurance, fat loss, and overall stamina [8,9]. In contrast, HIIT consists of alternating brief bursts of high-intensity exercise, such as sprints, with short recovery periods [10]. It provides fitness benefits within a shorter time frame, particularly in enhancing metabolism, fat loss, muscle strength, and cardiovascular function [11,12].

Although previous studies on MICT and HIIT have provided valuable insights into their distinct effects on physiological and functional outcomes [13,14], the molecular mechanisms governing skeletal muscle adaptation to these exercise modalities remain poorly explored. Bridging this gap is critical for understanding how different types of exercise shape muscle plasticity at the molecular level, paving the way for optimized training protocols and personalized exercise strategies. In particular, the growing recognition of exercise as a therapeutic intervention for a wide range of health conditions underscores the urgency of unraveling the transcriptional basis of muscle adaptation to different exercise types.

This study employs RNA-seq to characterize the transcriptomic profile of murine gastrocnemius muscle following an 8-week treadmill-based MICT/HIIT regimen. By elucidating the molecular pathways underpinning the distinct adaptations to these two modalities, this study contributes to a deeper understanding of skeletal muscle plasticity and provides valuable insights for sports science and therapeutic strategies.

Materials and methods

Animals

14-week-old male C57BL/6J mice were housed in SPF-grade rooms, with controlled temperature ($22^{\circ}\text{C} \pm 2^{\circ}\text{C}$) and humidity ($50\% \pm 5\%$). Mice were divided into three groups (each $n = 12$): sedentary control (C), MICT (M), and HIIT (H). All mice were purchased from Tsinghua Laboratory Resource Center. This study was approved by the Institutional Animal Care and Use Committee of Tsinghua University (Approval No: THU-LARC-2023-004) and was conducted in accordance with the ARRIVE guidelines. All animal methods were carried out in accordance with relevant guidelines and regulations.

Exercise protocol

MICT: Adaptation training was conducted for 1 week at a speed of 10 m/min for 15 minutes per day. Formal training was conducted for 8 weeks, with sessions lasting 45 minutes per day, five days a week. To monitor exercise intensity, a maximal oxygen uptake ($\text{VO}_{2\text{max}}$) test was conducted every two weeks using the TSE Systems Phenomaster (S1 Table). The MICT training regimen: 15 m/min for weeks 1-2, 17 m/min for weeks 3-4, and 19 m/min for weeks 5-8.

HIIT: Adaptation training was conducted for 1 week at a speed of 10 m/min for 15 minutes per day. Formal training was conducted for 8 weeks, five days a week. Each HIIT session consisted of 1 minute of high-intensity exercise (90% of $\text{VO}_{2\text{max}}$, 24 m/min for weeks 1-2, 26 m/min for weeks 3-4, 28 m/min for weeks 5-8) followed by 2 minutes of moderate-intensity exercise (60% of $\text{VO}_{2\text{max}}$, same as MICT). The number of HIIT repetitions was adjusted to match the total distance covered by the MICT group.

Body weight and serum parameter measurements

Body weight was measured and recorded weekly. Following intraperitoneal injection of Avertin for anesthesia, blood was drawn from the eye. Serum was separated by centrifugation at 3000 rpm for 15 minutes at 4°C , and serum triglyceride and glucose levels were quantified using an automated chemistry analyzer (Kehua ZY KHB1280).

Gastrocnemius muscle RNA-seq

RNA-seq was conducted at Biomarker (Beijing, China). Paired-end reads were quality checked and trimmed using Trim-galore (v.0.6.0). Alignment of the reads to the mouse genome reference (GRCm38.p6) from GENCODE was performed using STAR (v.2.7.3a). Subsequently, featureCounts (v.1.6.3) was utilized to count reads mapped to exon sites of genes listed in GTF files obtained from GENCODE. Differential expression analysis was carried out using DESeq2 (v.1.22.2), with raw counts as input. Functional enrichment analyses, including KEGG and GO analyses of differentially expressed genes (DEGs), were performed using clusterProfiler (v3.10.1).

Quantitative real-time PCR

Gastrocnemius muscle (each group $n = 6$) total RNA extraction was performed with Trizol (Invitrogen) according to the manufacturer's instructions. cDNA was synthesized using HiScript II Q RT SuperMix (Vazyme). Quantitative RT-PCR was performed using AceQ qPCR SYBR Green Master Mix (Vazyme). The experiment was independently repeated three times.

The following primers were used:

Gapdh Forward: AGAAGGTGGTGAAGCAGGCATCT
Reverse: CGGCATCGAAGGTGGAAGAGTG

Igf-1 Forward: CTGGACCAGAGACCCCTTTGC
Reverse: GGACGGGGACTTCTGAGTCTT

Sparc Forward: GTGGAAATGGGAGAATTTGAGGA
Reverse: CTCACACACCTTGCCATGTTT

Statistical analysis

GraphPad Prism 7 (Graphpad software) was used to assess statistical significance. The data are presented as $\bar{x} \pm s$. One-way analysis of variance (ANOVA) was used for comparisons between multiple groups followed by Tukey's post-hoc test, $p < 0.05$ was considered statistically significant.

Results

Physiological parameters

To investigate the transcriptional adaptation of skeletal muscle in response to MICT and HIIT, 14-week-old C57BL/6J mice were divided into three groups: sedentary control (C), MICT (M), HIIT (H). After grouping, the mice were initially weighed (referred to as week 1) and then underwent an 8-week treadmill MICT/HIIT regimen following a one-week adaptative training. As shown in [Table 1](#), the body weight of mice in each group remained relatively stable throughout the experimental period. Additionally, no significant differences were observed in blood glucose, blood triglyceride, gastrocnemius muscle mass and gastrocnemius muscle index (the ratio of bilateral gastrocnemius muscle weight to body weight) among the groups ([Table 2](#)).

Gene expression analysis

As shown in [Fig 1A](#), the principal components analysis (PCA) indicated clear separation among the C, M, and H groups, suggesting significant differences among the three groups and high consistency within each group.

Table 1. Body weight.

Week	C	M	H
1	30.1 ± 1.9	29.5 ± 1.6	28.9 ± 1.8
2	30.5 ± 1.8	30.1 ± 2.0	29.1 ± 1.6
3	31.1 ± 1.5	30.5 ± 1.7	29.0 ± 1.7
4	30.8 ± 1.6	30.2 ± 1.5	29.2 ± 1.7
5	30.2 ± 1.3	29.3 ± 1.7	29.2 ± 1.9
6	31.4 ± 1.7	30.2 ± 1.6	29.3 ± 2.2
7	30.9 ± 1.6	30.9 ± 1.9	29.9 ± 2.1
8	31.6 ± 2.0	31.2 ± 1.8	30.3 ± 2.1
9	31.3 ± 2.4	31.0 ± 2.1	31.1 ± 2.4

<https://doi.org/10.1371/journal.pone.0318782.t001>

Table 2. Physiological parameters.

Group	Blood glucose (mmol/L)	Blood triglyceride (mmol/L)	Gastrocnemius muscle mass (mg)	Gastrocnemius muscle index
C	14.526 ± 1.53	2.494 ± 0.22	182.4 ± 10.9	0.011438 ± 0.000537
M	14.025 ± 1.56	2.505 ± 0.20	185.3 ± 7.5	0.011638 ± 0.000785
H	13.531 ± 1.57	2.385 ± 0.30	181.0 ± 8.4	0.011730 ± 0.001346

<https://doi.org/10.1371/journal.pone.0318782.t002>

We applied a filtering criteria of adjusted p value < 0.05 and $|\log_2 \text{foldchange}| \geq 0.3$ for this study. In total, 2369 (1217 up-regulated, 1152 down-regulated), 2539 (1171 up-regulated, 1368 down-regulated) and 1052 (336 up-regulated, 716 down-regulated) DEGs were identified in M vs. C, H vs. C and H vs. M, respectively (Fig 1B, S2–S4 Tables). The expression of DEGs in the three groups for each comparison was presented using heatmap (Fig 1C).

The top 10 significant DEGs in M vs. C were *Ucp3*, *Galnt15*, *Slc7a8*, *Fkbp5*, *Rnf144b*, *Cep85l*, *Pkp4*, *Irs1*, *Xdh*, *Plin4* (Table 3). The top 10 significant DEGs in H vs. C were *Rnf144b*, *Galnt15*, *Plin4*, *Ucp3*, *Xdh*, *Rasal2*, *Cep85l*, *Pkp4*, *Glul*, *Plcb4* (Table 4). 7 out of 10 of the most significant DEGs in M vs. C were also detected in H vs. C (Fig 1D), suggesting a substantial overlap in the transcriptomic adaptation elicited by the two exercise modalities. The top 10 significant DEGs in H vs. M were *Apold1*, *Dusp10*, *Myod1*, *Ucp3*, *Fkbp5*, *Klf2*, *Zfp872*, *Plxna2*, *Ldlr*, *Foxo1* (Table 5).

GO functional classification

To elucidate the biological functions of these DEGs, we performed gene ontology (GO) functional classification. Using a q value threshold of less than 0.01, we identified 466, 255 and 54 significantly enriched terms in M vs. C, H vs. C and H vs. M, respectively.

In M vs. C, the top 15 significantly enriched terms (biological process) included positive regulation of kinase activity, regulation of ERK1 and ERK2 cascade, ERK1 and ERK2 cascade, ATP metabolic process, positive regulation of catabolic process, fat cell differentiation, vascular endothelial growth factor signaling pathway, regulation of sprouting angiogenesis, oxidative phosphorylation, cellular response to vascular endothelial growth factor stimulus, bone development, mesenchymal cell proliferation, regulation of fat cell differentiation, energy derivation by oxidation of organic compounds, positive regulation of cellular catabolic process (Fig 2A, S5 Table).

In H vs. C, the top 15 significantly enriched terms (biological process) were aerobic respiration, generation of precursor metabolites and energy, cellular respiration, oxidative

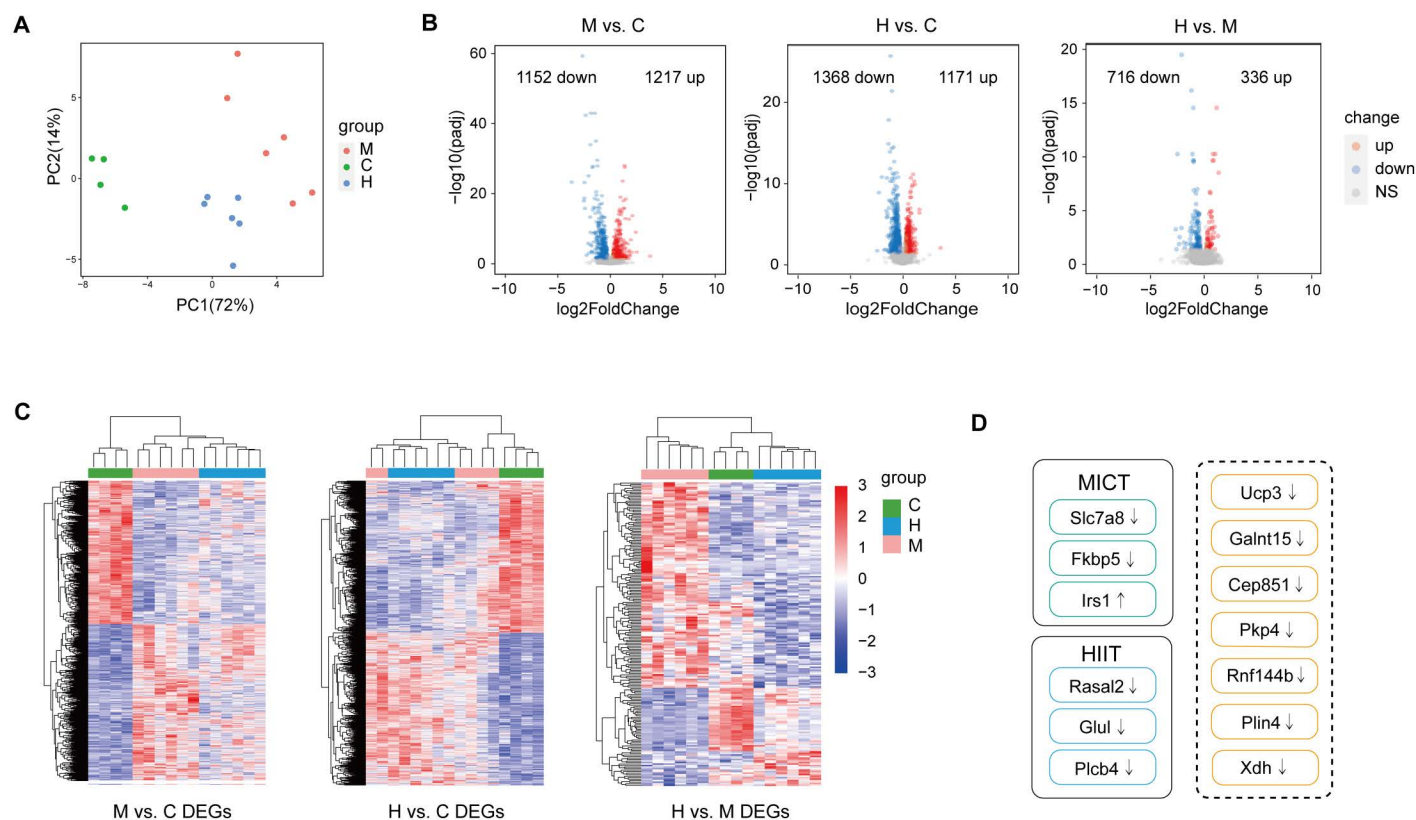


Fig 1. Gastrocnemius muscle transcriptome analysis. (A) PCA of total genes in C, M, H groups. (B) Volcano plots show DEGs in M vs. C, H vs. C and H vs. M. (C) Hierarchical clustering analysis of DEGs (M vs. C, H vs. C, H vs. M) in C, M, H groups. (D) The top 10 significant DEGs in M vs. C and H vs. C. Yellow indicates the common DEGs.

<https://doi.org/10.1371/journal.pone.0318782.g001>

Table 3. The top 10 significant DEGs in M vs. C.

Gene Symbol	Official Full Name	\log_2 (FC)	adjusted p value	Regulation
<i>Ucp3</i>	Uncoupling protein 3	-2.64243	1.22E-59	down
<i>Galnt15</i>	Polypeptide N-acetylgalactosaminyltransferase 15	-1.46987	2.05E-43	down
<i>Slc7a8</i>	Solute carrier family 7 member 8	-1.83976	2.05E-43	down
<i>Fkbp5</i>	FKBP prolyl isomerase 5	-2.33283	8.17E-43	down
<i>Rnf144b</i>	Ring finger protein 144B	-1.35914	1.59E-35	down
<i>Cep85l</i>	Centrosomal protein 85 like	-1.88382	1.75E-34	down
<i>Pkp4</i>	Plakophilin 4	-1.23892	4.37E-30	down
<i>Irs1</i>	Insulin receptor substrate 1	1.361908	1.34E-28	up
<i>Xdh</i>	Xanthine dehydrogenase	-1.20137	1.85E-28	down
<i>Plin4</i>	Perilipin 4	-1.6394	2.34E-28	down

<https://doi.org/10.1371/journal.pone.0318782.t003>

phosphorylation, energy derivation by oxidation of organic compounds, mitochondrial respiratory chain complex assembly, ATP metabolic process, NADH dehydrogenase complex assembly, mitochondrial respiratory chain complex I assembly, aerobic electron transport chain, mitochondrial ATP synthesis coupled electron transport, ATP synthesis coupled electron transport, respiratory electron transport chain, electron transport chain, mitochondrial electron transport NADH to ubiquinone (Fig 2B, S6 Table).

Table 4. The top 10 significant DEGs in H vs. C.

Gene Symbol	Official Full Name	log ₂ (FC)	adjusted p value	Regulation
<i>Rnf144b</i>	Ring finger protein 144B	-1.19462	1.98E-26	down
<i>Galnt15</i>	Polypeptide N-acetylgalactosaminyltransferase 15	-1.069	4.18E-22	down
<i>Plin4</i>	Perilipin 4	-1.35854	1.61E-18	down
<i>Ucp3</i>	Uncoupling protein 3	-1.39597	1.48E-15	down
<i>Xdh</i>	Xanthine dehydrogenase	-0.90166	3.69E-15	down
<i>Rasal2</i>	RAS protein activator like 2	-1.0771	5.26E-15	down
<i>Cep85l</i>	Centrosomal protein 85 like	-1.2584	1.44E-14	down
<i>Pkp4</i>	Plakophilin 4	-0.84769	2.35E-13	down
<i>Glul</i>	Glutamate-ammonia ligase	-1.2254	1.69E-12	down
<i>Plcb4</i>	Phospholipase C beta 4	-0.62484	5.60E-12	down

<https://doi.org/10.1371/journal.pone.0318782.t004>

Table 5. The top 10 significant DEGs in H vs. M.

Gene Symbol	Official Full Name	log ₂ (FC)	adjusted p value	Regulation
<i>Apold1</i>	Apolipoprotein L domain containing 1	-2.04152	2.55E-20	down
<i>Dusp10</i>	Dual specificity phosphatase 10	-1.11973	5.72E-17	down
<i>Myod1</i>	Myogenic differentiation 1	-0.94908	2.45E-15	down
<i>Ucp3</i>	Uncoupling protein 3	1.246461	2.46E-15	up
<i>Fkbp5</i>	FKBP prolyl isomerase 5	1.120498	5.37E-11	up
<i>Klf2</i>	KLF transcription factor 2	-1.02768	5.37E-11	down
<i>Zfp872</i>	Zinc finger protein 872	-2.42528	5.37E-11	down
<i>Plxna2</i>	Plexin A2	0.901478	5.42E-11	up
<i>Ldlr</i>	Low density lipoprotein receptor	-0.94415	2.18E-10	down
<i>Foxo1</i>	Forkhead box O1	0.972113	2.18E-10	down

<https://doi.org/10.1371/journal.pone.0318782.t005>

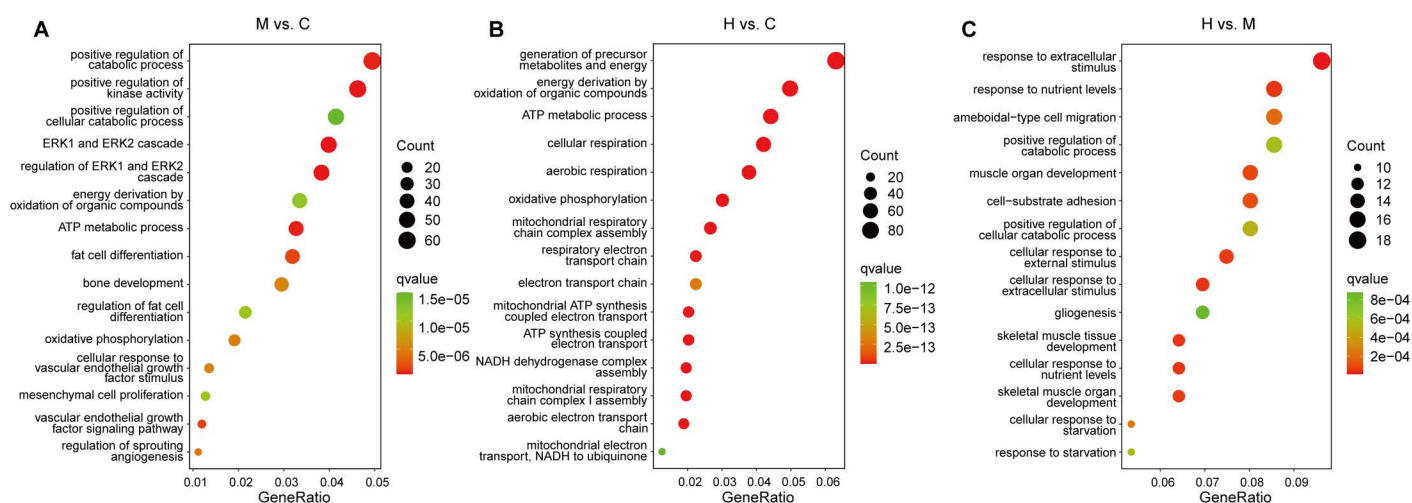


Fig 2. GO function classification (biological process) of DEGs. (A) M vs. C, (B) H vs. C, (C) H vs. M.

<https://doi.org/10.1371/journal.pone.0318782.g002>

In H vs. M, the top 15 significantly enriched terms (biological process) included response to extracellular stimulus, response to nutrient levels, cellular response to extracellular stimulus, skeletal muscle tissue development, cellular response to nutrient levels, skeletal muscle organ development, cellular response to external stimulus, muscle organ development, cell-substrate adhesion, amoeboid-type cell migration, cellular response to starvation, positive regulation of cellular catabolic process, response to starvation, positive regulation of catabolic process, gliogenesis (Fig 2C, S7 Table).

KEGG pathway analysis

To deepen our comprehension of these DEGs, we employed Kyoto Encyclopedia of Genes and Genomes (KEGG) pathway analysis to elucidate their roles in biological pathways. Using a q-value threshold of less than 0.05, we identified significant enrichment of 46, 45, and 4 pathways in M vs. C, H vs. C, and H vs. M, respectively.

In M vs. C, the top 15 significantly enriched pathways were prion disease, diabetic cardiomyopathy, Parkinson disease, Rap1 signaling pathway, circadian rhythm, Ras signaling pathway, chemical carcinogenesis-reactive oxygen species, EGFR tyrosine kinase inhibitor resistance, Huntington disease, thyroid hormone signaling pathway, focal adhesion, non-alcoholic fatty liver disease, Alzheimer disease, thermogenesis, apoptosis (Fig 3A and S8 Table).

In H vs. C, the top 15 significantly enriched pathways included oxidative phosphorylation, chemical carcinogenesis-reactive oxygen species, Parkinson disease, thermogenesis, diabetic cardiomyopathy, Huntington disease, prion disease, Alzheimer disease, amyotrophic lateral sclerosis, non-alcoholic fatty liver disease, pathways of neurodegeneration, retrograde endocannabinoid signaling, circadian rhythm, gap junction, carbon metabolism (Fig 3B and S9 Table).

In H vs. M, the significantly enriched pathways were FoxO signaling pathway, longevity regulating pathway, insulin resistance, MAPK signaling pathway (Fig 3C and S10 Table).

Myokines and muscle fiber markers

Myokines, produced by skeletal muscle cells, represent a class of cytokines or peptides [15]. Research has suggested that myokines play pivotal roles in modulating inflammation, lipid

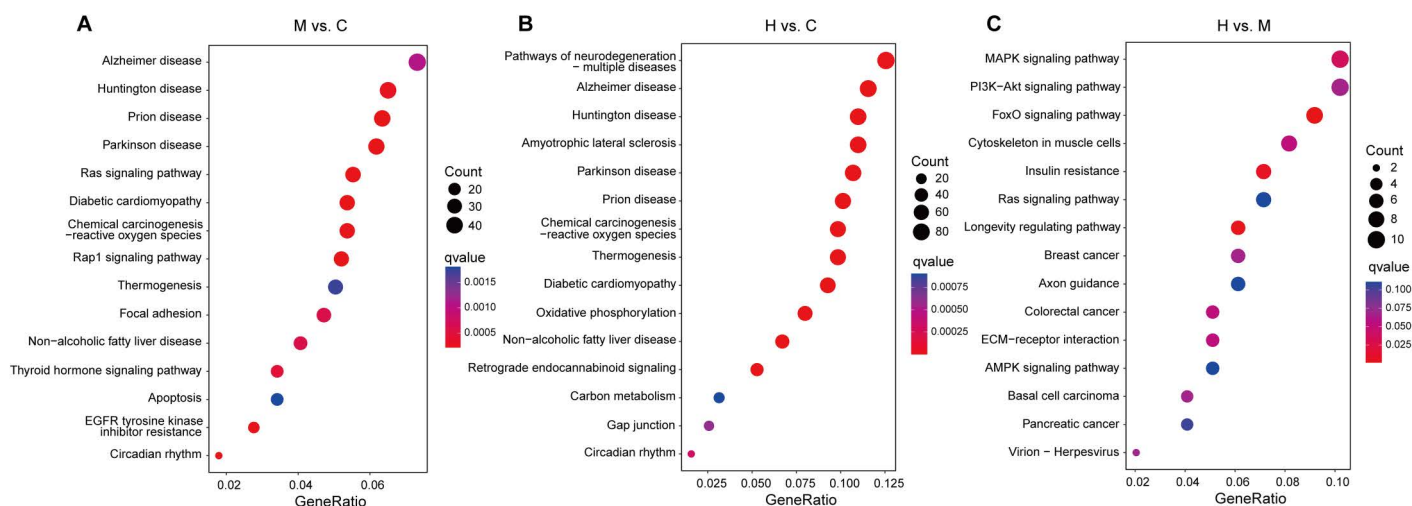


Fig 3. KEGG pathway analysis of DEGs. (A) M vs. C, (B) H vs. C, (C) H vs. M.

<https://doi.org/10.1371/journal.pone.0318782.g003>

metabolism, energy metabolism, and overall health [16,17]. Therefore, we analyzed the expression levels of various myokines, including adiponectin (*Adipoq*), decorin (*Dcn*), myostatin (*Mstn*), fibronectin type III domain-containing protein 5 (*Fndc5*), insulin-like growth factor 1 (*Igf1*), interleukin 15 (*Il15*), secreted protein acidic and rich in cysteine (*Sparc*), growth differentiation factor 11 (*Gdf11*), and osteonectin (*Ostn*). Among these, the expression levels of *Igf-1* and *Sparc* were significantly different between the two exercise modalities (Fig 4A). Subsequently, we analyzed the expression levels of various markers of muscle fiber: *Myh1* (IIX), *Myh2* (IIA), *Myh4* (IIB), *Myh7* (I), *Myl1* (II), *Myl2* (I), *Myl3* (I), *Myl6b* (I), and *Mylpf* (II). There was no notable variance between the two exercise modalities (Fig 4B). Furthermore, quantitative RT-PCR was performed to validate the RNA-seq results. Consistently, *Igf-1* mRNA level was significantly higher in the M group compared to the H group, while no significant difference was observed in *Sparc* mRNA expression (Fig 4C).

Discussion

Skeletal muscle, as the primary organ responsible for movement, plays a critical role during physical activity. Its adaptive changes in response to exercise not only manifest as alterations in muscle structure and function but also entail genetic regulation and adaptation [18,19]. Understanding how skeletal muscle adapts at the genetic level to different types of exercise is crucial for optimizing training strategies and improving health outcomes.

In this study, we investigated the effects of 8 weeks of treadmill-based MICT and HIIT on the transcriptome of murine skeletal muscle. No significant differences in body weight, glucose and triglycerides were observed between the C group and exercise groups. This was likely attributed to the use of 14-week-old C57BL/6J mice. At this age, mice have achieved stable body weight and metabolic homeostasis, making them a suitable model for studying skeletal muscle adaptations to exercise while minimizing potential confounding effects related to development.

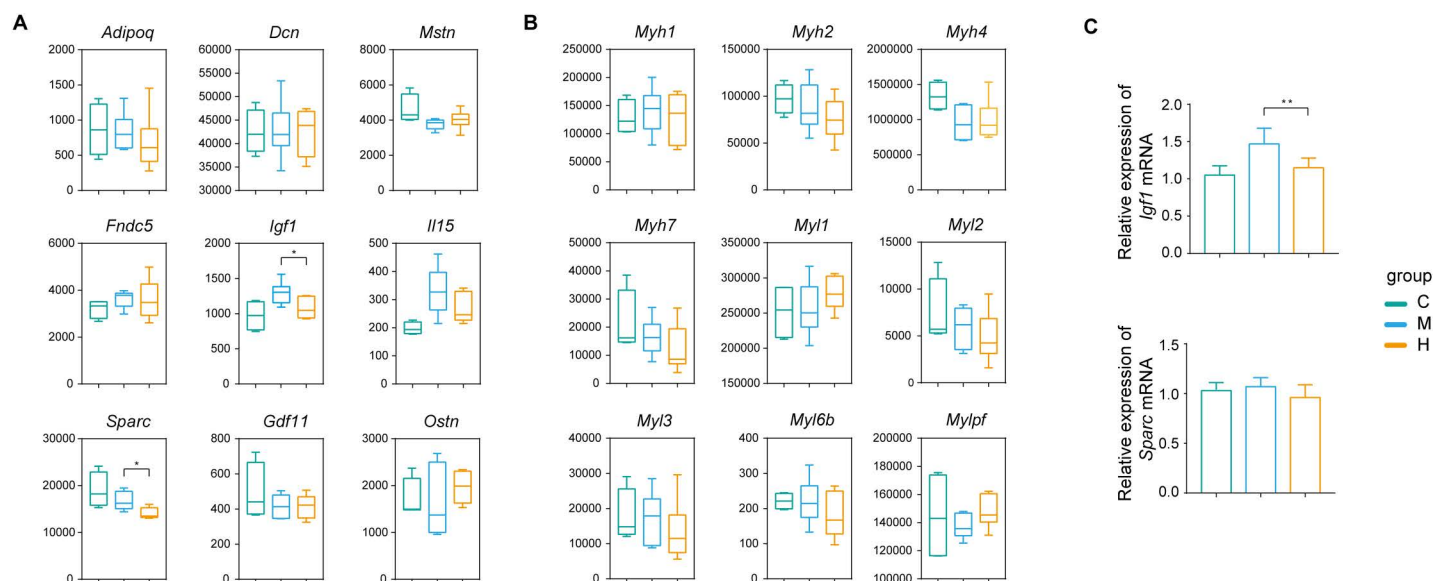


Fig 4. The expression levels of myokines and muscle fiber markers. (A) The expression levels (RNA-seq counts) of myokines and (B) muscle fiber markers in C, M, H groups. (C) Expression of *Igf-1* and *Sparc* mRNA in C, M, H, groups' gastrocnemius muscle (each group n = 6); results are shown as relative expression normalized to that of *Gapdh* mRNA. * $p < 0.05$, ** $p < 0.01$.

<https://doi.org/10.1371/journal.pone.0318782.g004>

Applying the filtering criteria of adjusted p value < 0.05 and $|\log_2 \text{foldchange}| \geq 0.3$, 1052 DEGs were identified in H vs. M. Among the top 10 significant DEGs, *Foxo1* (mean counts: C, 4616; M, 1413; H, 2772) is of particular interest. FoxO1 is a transcription factor that regulates the expression of genes involved in muscle protein degradation and cellular processes associated with muscle wasting, such as autophagy and the ubiquitin-proteasome system [20]. Target genes of FoxO1 in muscle atrophy include those encoding for proteins involved in muscle protein breakdown, such as *Murf1* (muscle-specific RING finger protein 1) and *Atrogin-1*, as well as genes related to autophagy and oxidative stress response [21,22]. Increased FoxO1 activity is a hallmark of muscle atrophy, contributing to the breakdown of muscle proteins and leading to a loss of muscle mass and function [23]. Activated AKT phosphorylates FoxO1 directly, leading to its exclusion from the nucleus, thus inhibiting FoxO1's transcriptional activity. Other significant DEG related to muscular physiology is *Myod1* (mean counts: C, 529; M, 1390; H, 720). MyoD is a member of the myogenic regulatory factors (MRFs) family, which plays a critical role in muscle development and regeneration [24]. As a transcription factor, MyoD regulates the expression of genes involved in muscle differentiation, including those encoding structural proteins essential for muscle formation. It acts as a master regulator by activating the muscle-specific gene program and promoting the conversion of undifferentiated cells into muscle cells (myoblasts) [25]. MyoD is particularly important during embryonic development for the initial specification of skeletal muscle lineage and in adult skeletal muscle for the repair and regeneration of damaged muscle tissue [26].

Beyond the gene level, GO functional classification revealed that the majority of DEGs in H vs. M were associated with extracellular stimulus, nutrient levels, and skeletal muscle development. The significantly enriched pathways in H vs. M were FoxO signaling pathway, longevity regulating pathway, insulin resistance, MAPK signaling pathway. Interestingly, these pathways are closely associated with PI3K-AKT pathway and its upstream regulator, IGF-1 [27]. IGF-1, a protein hormone structurally akin to insulin, profoundly contributes to muscle growth, repair, and regeneration by acting as a potent stimulator of muscle protein synthesis [28,29]. It interacts specifically with the IGF receptor situated on the cell surface, initiating a cascade of events. Upon ligand binding, the receptor undergoes a conformational change in its β subunit, activating its tyrosine kinase activity. Consequently, the activated receptor phosphorylates various substrates, including insulin receptor substrates (IRSs) and Src homology collagen (SHC) proteins. These substrates, in turn, initiate two primary intracellular signaling pathways: the PI3K/AKT pathway and the MAPK pathway.

While IGF-1 is primarily synthesized in the liver and released into the bloodstream, muscle tissue also produces and secretes IGF-1 [30]. In muscle tissue, the synthesis of IGF-1 is regulated by stimulation (e.g., exercise [31]). We found that the expression level of *Igf-1* in M group was significantly higher than that in H group (Fig 4A,C). As depicted in Fig 5, several key components of IGF1-PI3K-AKT pathway were also expressed at higher levels in M group, indicating a potentially heightened activation of IGF1-PI3K-AKT pathway induced by MICT. Since it has been reported that downregulation of IGF1-PI3K-AKT signaling pathway and increased FoxO activity were often associated with muscle atrophy in diseased states or in elderly individuals [32–34], our findings suggest that MICT might offer superior benefits compared to HIIT in ameliorating muscle atrophy under such conditions.

Limitations: One limitation of this study is the relatively small sample size ($n = 12$ per group), which may reduce the statistical power to detect subtle differences and increase the potential impact of individual variability in exercise response. Future studies with larger sample sizes are necessary to validate these findings and ensure greater generalizability.

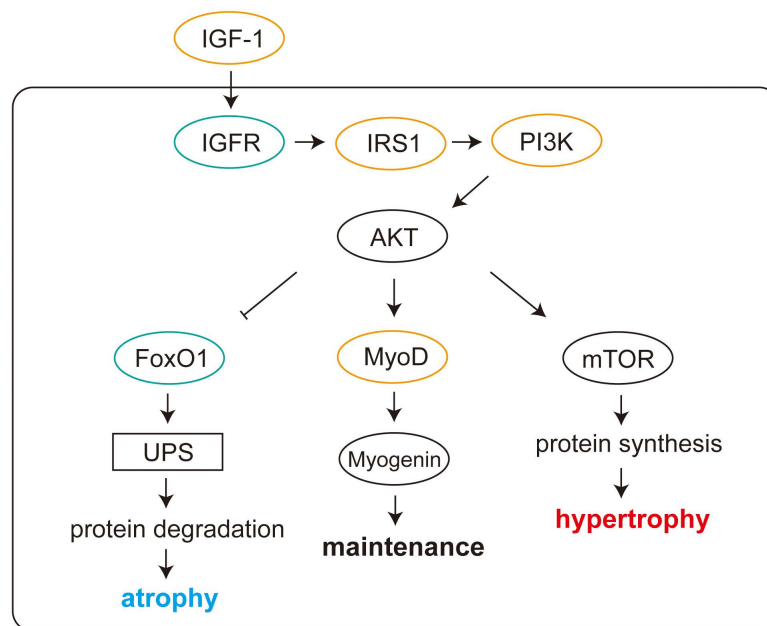


Fig 5. IGF1-PI3K-AKT pathway. orange/green indicates significantly higher/lower expression levels in M group than that in H group. UPS, ubiquitin-proteasome system.

<https://doi.org/10.1371/journal.pone.0318782.g005>

Additionally, the use of a murine model, while informative, may not fully replicate the adaptive responses in human skeletal muscle due to species-specific differences. Validation of these findings in human models or across different age groups would further enhance the applicability of the results.

The intervention lasted only 8 weeks, which, while sufficient to observe short-term transcriptomic adaptations, may not capture the full extent of long-term effects, such as sustained improvements in muscle function or metabolic health. Future studies with extended training durations are needed to better elucidate these longer-term adaptations.

Furthermore, the exercise volume in this study was controlled by keeping the running distance constant across groups. However, exercise intensity, duration, and distance are all critical variables that can influence adaptive outcomes. By focusing on a fixed distance, this study may have overlooked the broader spectrum of responses that could result from variations in these parameters, especially differences in energy expenditure or recovery dynamics between the exercise modalities.

Lastly, this study relied exclusively on transcriptomic analysis, which provides valuable insights into gene expression changes but does not directly capture post-transcriptional modifications, protein abundance, or metabolite interactions. Integrating proteomic and metabolomic analyses in future studies could offer a more comprehensive understanding of the molecular mechanisms underlying skeletal muscle adaptations to different exercise modalities.

Conclusions

This study sheds light on the transcriptomic landscape of skeletal muscle in response to MICT and HIIT, highlighting distinct adaptations in the FoxO, MAPK, and PI3K-AKT signaling pathways. These differences might be attributed to variations in *Igf-1* expression elicited by the two exercise modalities.

Supporting information

S1 Table. VO₂max test.
(DOCX)

S2 Table. Deseq2 result M vs. C.
(CSV)

S3 Table. Deseq2 result H vs. C.
(CSV)

S4 Table. Deseq2 result H vs. M.
(CSV)

S5 Table. GO result M vs. C.
(CSV)

S6 Table. GO result H vs. C.
(CSV)

S7 Table. GO result H vs. M.
(CSV)

S8 Table. KEGG result M vs. C.
(CSV)

S9 Table. KEGG result H vs. C.
(CSV)

S10 Table. KEGG result H vs. M.
(CSV)

Author contributions

Conceptualization: Weihao Hong.

Formal analysis: Weihao Hong.

Funding acquisition: Bing Zhang, Yixuan Ma.

Investigation: Weihao Hong, Yisheng Luan, Yingzhe Xiong.

Methodology: Jianrong Zheng.

Resources: Yixuan Ma.

Supervision: Bing Zhang.

Validation: Weihao Hong.

Visualization: Weihao Hong.

Writing – original draft: Weihao Hong.

Writing – review & editing: Weihao Hong, Yingzhe Xiong, Bing Zhang, Yixuan Ma.

References

1. Kissane RWP, Hauton D, Tickle PG, Egginton S. Skeletal muscle adaptation to indirect electrical stimulation: divergence between microvascular and metabolic adaptations. *Exp Physiol.* 2023;108(6):891–911. Epub 2023/04/08. <https://doi.org/10.1113/EP091134> PMID: [37026596](#); PMCID: PMCPMC10988499
2. Smith JAB, Murach KA, Dyar KA, Zierath JR. Exercise metabolism and adaptation in skeletal muscle. *Nat Rev Mol Cell Biol.* 2023;24(9):607–32. Epub 2023/05/25. <https://doi.org/10.1038/s41580-023-00606-x> PMID: [37225892](#); PMCID: PMCPMC10527431

3. Camera DM, Smiles WJ, Hawley JA. Exercise-induced skeletal muscle signaling pathways and human athletic performance. *Free Radic Biol Med*. 2016;98:131–43. Epub 2016/02/16. <https://doi.org/10.1016/j.freeradbiomed.2016.02.007> PMID: 26876650
4. Egan B, Sharples AP. Molecular responses to acute exercise and their relevance for adaptations in skeletal muscle to exercise training. *Physiol Rev*. 2023;103(3):2057–170. Epub 2022/11/18. <https://doi.org/10.1152/physrev.00054.2021> PMID: 36395350
5. Dickinson JM, D'Lugos AC, Naymik MA, Siniard AL, Wolfe AJ, Curtis DR, et al. Transcriptome response of human skeletal muscle to divergent exercise stimuli. *J Appl Physiol* (1985). 2018;124(6):1529–40. Epub 2018/03/16. <https://doi.org/10.1152/jappphysiol.00014.2018> PMID: 29543133
6. Pillon NJ, Gabriel BM, Dollet L, Smith JAB, Sardón Puig L, Botella J, et al. Transcriptomic profiling of skeletal muscle adaptations to exercise and inactivity. *Nat Commun*. 2020;11(1):470. Epub 2020/01/26. <https://doi.org/10.1038/s41467-019-13869-w> PMID: 31980607; PMCID: PMC6981202
7. Wu W-D, Wang Y, Wei J-X. Effects of MICT/HIIT on the ultrastructure of myocardium and soleus in rats with high-fat diet and its mechanisms. *Zhongguo Ying Yong Sheng Li Xue Za Zhi*. 2022;38(6):708–13. Epub 2023/06/13. <https://doi.org/10.12047/j.cjap.6191.2022.129> PMID: 37308422
8. Seals DR, Nagy EE, Moreau KL. Aerobic exercise training and vascular function with ageing in healthy men and women. *J Physiol*. 2019;597(19):4901–14. Epub 2019/05/12. <https://doi.org/10.1113/JP277764> PMID: 31077372; PMCID: PMC6773490
9. Muscella A, Stefano E, Lunetti P, Capobianco L, Marsigliante S. The regulation of fat metabolism during aerobic exercise. *Biomolecules*. 2020;10(12):1699. Epub 2020/12/30. <https://doi.org/10.3390/biom10121699> PMID: 33371437; PMCID: PMC6776423
10. Coates AM, Joyner MJ, Little JP, Jones AM, Gibala MJ. A perspective on high-intensity interval training for performance and health. *Sports Med*. 2023;53(Suppl 1):85–96. Epub 2023/10/07. <https://doi.org/10.1007/s40279-023-01938-6> PMID: 37804419; PMCID: PMC6776423
11. Jelleyman C, Yates T, O'Donovan G, Gray LJ, King JA, Khunti K, et al. The effects of high-intensity interval training on glucose regulation and insulin resistance: a meta-analysis. *Obes Rev*. 2015;16(11):942–61. Epub 2015/10/21. <https://doi.org/10.1111/obr.12317> PMID: 26481101
12. Wang C, Xing J, Zhao B, Wang Y, Zhang L, Wang Y, et al. The effects of high-intensity interval training on exercise capacity and prognosis in heart failure and coronary artery disease: a systematic review and meta-analysis. *Cardiovasc Ther*. 2022;2022:4273809. Epub 2022/07/09. <https://doi.org/10.1155/2022/4273809> PMID: 35801132; PMCID: PMC6776423
13. Sini ZK, Afzalpour ME, Ahmadi MM, Sardar MA, Khaleghzadeh H, Gorgani-Firuzjaee S, et al. Comparison of the effects of high-intensity interval training and moderate-intensity continuous training on indices of liver and muscle tissue in high-fat diet-induced male rats with non-alcoholic fatty liver disease. *Egypt Liver J*. 2022;12(1). <https://doi.org/10.1186/s43066-022-00229-5>
14. Bhammar DM, Gaesser GA, et al. Effects of high-intensity interval training and moderate-intensity continuous training on endothelial function and cardiometabolic risk markers in obese adults. *J Appl Physiol*. 2016;121(1):279–88. <https://doi.org/10.1152/jappphysiol.00024.2016> PMID: 27255523
15. Zhang L, Lv J, Wang C, Ren Y, Yong M. Myokine, a key cytokine for physical exercise to alleviate sarcopenic obesity. *Mol Biol Rep*. 2023;50(3):2723–34. Epub 2022/12/27. <https://doi.org/10.1007/s11033-022-07821-3> PMID: 36571655
16. Huang Q, Wu M, Wu X, Zhang Y, Xia Y. Muscle-to-tumor crosstalk: the effect of exercise-induced myokine on cancer progression. *Biochim Biophys Acta Rev Cancer*. 2022;1877(5):188761. Epub 2022/07/20. <https://doi.org/10.1016/j.bbcan.2022.188761> PMID: 35850277
17. Severinsen MCK, Pedersen BK. Muscle-organ crosstalk: the emerging roles of myokines. *Endocr Rev*. 2020;41(4):594–609. Epub 2020/05/13. <https://doi.org/10.1210/endrev/bnaa016> PMID: 32393961; PMCID: PMC6776423
18. Viggars MR, Sutherland H, Lanmüller H, Schmoll M, Bijak M, Jarvis JC. Adaptation of the transcriptional response to resistance exercise over 4 weeks of daily training. *FASEB J*. 2023;37(1):e22686. Epub 2022/12/06. <https://doi.org/10.1096/fj.202201418R> PMID: 36468768
19. Group MS, Analysts L, Group MS. Temporal dynamics of the multi-omic response to endurance exercise training. *Nature*. 2024;629(8010):174–83. Epub 2024/05/02. <https://doi.org/10.1038/s41586-023-06877-w> PMID: 38693412
20. Vilchinskaya N, Altaeva E, Lomonosova Y. Gaining insight into the role of FoxO1 in the progression of disuse-induced skeletal muscle atrophy. *Adv Biol Regul*. 2022;85:100903. Epub 2022/08/11. <https://doi.org/10.1016/j.jbior.2022.100903> PMID: 35947892

21. Milan G, Romanello V, Pescatore F, Armani A, Paik J-H, Frasson L, et al. Regulation of autophagy and the ubiquitin-proteasome system by the FoxO transcriptional network during muscle atrophy. *Nat Commun*. 2015;6:6670. Epub 2015/04/11. <https://doi.org/10.1038/ncomms7670> PMID: [25858807](#); PMCID: PMC4403316
22. Hirose Y, Onishi T, Miura S, Hatazawa Y, Kamei Y. Vitamin D attenuates FOXO1-target atrophy gene expression in C2C12 muscle cells. *J Nutr Sci Vitaminol (Tokyo)*. 2018;64(3):229–32. Epub 2018/07/03. <https://doi.org/10.3177/jnsv.64.229> PMID: [29962435](#)
23. Brocca L, Toniolo L, Reggiani C, Bottinelli R, Sandri M, Pellegrino MA. FoxO-dependent atrogenes vary among catabolic conditions and play a key role in muscle atrophy induced by hindlimb suspension. *J Physiol*. 2017;595(4):1143–58. Epub 2016/10/22. <https://doi.org/10.1113/JP273097> PMID: [27767211](#); PMCID: PMC45309360
24. Hernández-Hernández JM, García-González EG, Brun CE, Rudnicki MA. The myogenic regulatory factors, determinants of muscle development, cell identity and regeneration. *Semin Cell Dev Biol*. 2017;72:10–8. Epub 2017/11/12. <https://doi.org/10.1016/j.semcdb.2017.11.010> PMID: [29127045](#); PMCID: PMC5723221
25. Shenoy PS, Bose B, Sharma M, McFarlane C, Kambadur R. Lack of myostatin reduces MyoD induced myogenic potential of primary muscle fibroblasts. *J Cell Biochem*. 2014;115(11):1908–17. Epub 2014/06/10. <https://doi.org/10.1002/jcb.24860> PMID: [24909401](#)
26. Cho OH, Mallappa C, Hernández-Hernández JM, Rivera-Pérez JA, Imbalzano AN. Contrasting roles for MyoD in organizing myogenic promoter structures during embryonic skeletal muscle development. *Dev Dyn*. 2015;244(1):43–55. Epub 2014/10/21. <https://doi.org/10.1002/dvdy.24217> PMID: [25329411](#); PMCID: PMC4276533
27. Kasprzak A. Insulin-like growth factor 1 (IGF-1) signaling in glucose metabolism in colorectal cancer. *Int J Mol Sci*. 2021;22(12):6434. Epub 2021/07/03. <https://doi.org/10.3390/ijms22126434> PMID: [34208601](#); PMCID: PMC8234711
28. Yoshida T, Delafontaine P. Mechanisms of IGF-1-mediated regulation of skeletal muscle hypertrophy and atrophy. *Cells*. 2020;9(9):1970. Epub 2020/08/30. <https://doi.org/10.3390/cells9091970> PMID: [32858949](#); PMCID: PMC7564605
29. Biagetti B, Simó R. GH/IGF-1 abnormalities and muscle impairment: from basic research to clinical practice. *Int J Mol Sci*. 2021;22(1):415. Epub 2021/01/07. <https://doi.org/10.3390/ijms22010415> PMID: [33401779](#); PMCID: PMC7795003
30. Gomasca M, Banfi G, Lombardi G. Myokines: the endocrine coupling of skeletal muscle and bone. *Adv Clin Chem*. 2020;94:155–218. Epub 2020/01/19. <https://doi.org/10.1016/bs.acc.2019.07.010> PMID: [31952571](#)
31. Feng L, Li B, Xi Y, Cai M, Tian Z. Aerobic exercise and resistance exercise alleviate skeletal muscle atrophy through IGF-1/IGF-1R-PI3K/Akt pathway in mice with myocardial infarction. *Am J Physiol Cell Physiol*. 2022;322(2):C164–76. Epub 2021/12/02. <https://doi.org/10.1152/ajpcell.00344.2021> PMID: [34852207](#)
32. Jun L, Robinson M, Geetha T, Broderick TL, Babu JR. Prevalence and mechanisms of skeletal muscle atrophy in metabolic conditions. *Int J Mol Sci*. 2023;24(3):2973. Epub 2023/02/12. <https://doi.org/10.3390/ijms24032973> PMID: [36769296](#); PMCID: PMC9917738
33. Chen K, Gao P, Li Z, Dai A, Yang M, Chen S, et al. Forkhead box O signaling pathway in skeletal muscle atrophy. *Am J Pathol*. 2022;192(12):1648–57. Epub 2022/09/30. <https://doi.org/10.1016/j.ajpath.2022.09.003> PMID: [36174679](#)
34. Malavaki CJ, Sakkas GK, Mitrou GI, Kalyva A, Stefanidis I, Myburgh KH, et al. Skeletal muscle atrophy: disease-induced mechanisms may mask disuse atrophy. *J Muscle Res Cell Motil*. 2015;36(6):405–21. Epub 2016/01/06. <https://doi.org/10.1007/s10974-015-9439-8> PMID: [26728748](#)